

Hyperthermotherapy enhances antitumor effect of 5-aminolevulinic acid-mediated sonodynamic therapy with activation of caspase-dependent apoptotic pathway in human glioma

Donghui Ju^{1,2} · Fumio Yamaguchi² · Guangzhi Zhan² · Tadashi Higuchi² · Takayuki Asakura² · Akio Morita² · Hideo Orimo³ · Shaoshan Hu¹

Received: 23 November 2015 / Accepted: 28 January 2016 / Published online: 4 February 2016
© International Society of Oncology and BioMarkers (ISOBM) 2016

Abstract Sonodynamic therapy (SDT) has shown great potential as an approach for cancer treatment, and hyperthermotherapy (HT) is also a promising cancer therapy. Here, we investigate whether HT could improve the efficacy of SDT and to make a preliminary exploration on potential mechanism. Xenograft tumor was established in nude mice model, and SNB19 and U87MG glioma cell lines were utilized for in vitro experiment. Alamar blue assay was performed to assess cell viability. Optical microscope was used to characterize the morphology changes of the glioma cells induced by SDT and HT treatments. Apoptotic rate, mitochondrial membrane potential (MMP), and intracellular production of reactive oxygen species (ROS) were examined by flow cytometer. The cell apoptosis of tumor tissues were detected by TUNEL assay. Furthermore, the expression of apoptosis-related proteins was detected with Western blot in vitro and immunohistochemistry in vivo. SDT plus HT group could significantly reduce the cell viability with circular-cell morphological change, compared with SDT group, and cell viability was decreased depending on raise of 5-ALA concentration, ultrasound exposure time, and temperature. The results also indicate that HT increased a conspicuous apoptosis, ROS

production, and a remarkable loss in MMP induced by 5-ALA-SDT in vitro. Meanwhile, our data also demonstrated that the combined treatment could significantly induce apoptosis and delay tumor growth in vivo. Furthermore, in both in vitro and in vivo experiments, SDT plus HT group expressed significantly higher protein levels of Bax and cleaved caspase-3, 8, and 9 compared to SDT, HT, and control groups and significantly lower protein level of bcl-2 than the other three groups, while the expression of these proteins was unchanged between HT and control groups. HT may provide an important promotion on 5-ALA-SDT and further propose that SDT in combination with HT is a new potential application for the treatment of human glioma.

Keywords Sonodynamic therapy · 5-aminolevulinic acid · Hyperthermotherapy · Antitumor effect · Apoptosis · Glioma

Introduction

As the most common primary malignant brain tumor, glioma is characterized by rapid proliferation, strong invasiveness, unsatisfactory prognosis, and so forth [1–3]. The median survival for glioblastoma patients is still at a mere 14 months even under multidisciplinary treatments like tumor resection, radiotherapy, and chemotherapy [4, 5]. To conquer this hard problem, new promising and more effective treatments have been constantly explored [5–7].

Some investigators advocated treating cancer with hyperthermotherapy (HT) [8–10], which creates a promising approach to cancer therapy. Heating cancer cells at 42 °C or higher temperature can be pretty effective due to tumor cells' specific sensitivity [8, 11, 12]. Technically, HT works through destroying the structure of cytomembrane, activating

✉ Shaoshan Hu
shaoshanhu@126.com

¹ Department of Neurosurgery, The Second Affiliated Hospital of Harbin Medical University, Harbin 150086, China

² Department of Neurological Surgery, Nippon Medical School, 1-1-5 Sendagi, Bunkyo-ku, Tokyo 113-8603, Japan

³ Division of Metabolism and Nutrition, Department of Biochemistry and Molecular Biology, Nippon Medical School, 1-1-5 Sendagi, Bunkyo-ku, Tokyo 113-8602, Japan

lysosomes, inhibiting the synthesis of DNA, RNA, and protein, and inducing protein denaturation [8, 13, 14]. However, HT exerts a mild effect on antitumor. A synergistic administration with other therapies is expected to be more effective.

It is well known that 5-aminolevulinic acid (5-ALA), a metabolic precursor of protoporphyrin IX (PpIX) in the heme biosynthesis pathway, has a specific accumulation in the tumor tissue [15]. In most studies, 5-ALA has been widely used as a photosensitizer or sonosensitizer in photodynamic therapy (PDT) and sonodynamic therapy (SDT) on many human tumors including malignant glioma [16–18]. As a relatively novel and noninvasive approach to cancer treatment on the basis of photodynamic therapy, SDT is first proposed by Umemura et al. in 1990 [19]. With ultrasound, SDT has a strong ability to penetrate biological tissue. In particular, focused ultrasound can gather the sound power to the deeper tissue and activate certain sonosensitizers, thus having the antitumor effect [20, 21]. Recent research suggests that SDT is fairly effective in killing glioma. It has been reported that many mechanisms had been put forward to describe the antitumor effect of SDT, mainly including ultrasonic cavitation, reactive oxygen species (ROS) causing cell damage, inducing apoptosis and autophagy, and so on [20–23].

However, given their respective anticancer effect and mechanism, it still remains unclear whether the combined application of SDT and HT will lead to a stronger effect. Therefore, it is essential to investigate its antitumor effect and mechanism. And it will contribute to the evolution of anti-glioma therapy. To the best of our knowledge, there has been no similar study reported in the English literature to date. As such, in our research, we aimed to investigate human malignant glioma reaction by SDT in conjunction with HT, by evaluating cell apoptosis, mitochondrial membrane potential (MMP), and intracellular production of reactive oxygen species (ROS) *in vitro* and tumor growth *in vivo* and to make a preliminary exploration on potential mechanism.

Materials and methods

Chemicals and reagents

5-aminolevulinic acid was purchased from Cosmo BioCo., Ltd. (Tokyo, Japan) and was dissolved in 1 N HCL solution to make a 100 mM stock solution. One hundred-millimeter stock solution was sterilized, aliquoted, and stored at -80°C in the dark. Dulbecco's modified Eagle's medium (DMEM), fetal bovine serum (FBS), streptomycin, and penicillin were obtained from Gibco (Grand Island, NY, USA). Alamar Blue® and MitoProbe™ DiIC1(5) Assay Kit for Flow Cytometry were from Invitrogen (Carlsbad, CA, USA). CellROX® Green Flow Cytometry Assay Kit was purchased from Life Technologies (Eugene, Oregon, USA). Annexin V-

FITC Apoptosis Detection Kit was obtained from Beyotime (Shanghai, China).

Cell lines and cell culture

SNB19 is a well-characterized human glioblastoma cell line [24]. U87MG, another human primary glioblastoma cell line, was purchased from ATCC (American Type Culture Collection, Manassas, VA, USA). The human glioma cell lines SNB19 and U87MG were cultured in DMEM containing 10 % fetal bovine serum, 100 U/ml penicillin, and 100 $\mu\text{g}/\text{ml}$ streptomycin at 37°C in a humidified incubator with atmosphere of 5 % CO_2 . The cells were harvested for passage twice per week when they were nearly confluent.

SDT and HT procedure *in vitro*

The ultrasound device used in this study, which is composed of ultrasonic electronic generator, amplifier and transducer, was manufactured by Ito CO., LTD (Tokyo, Japan), as is shown in Fig. 1. The ultrasound transducer (diameter: 3.5 cm, resonance frequency: 1.0 MHz, duty factor: 20 %, ultrasonic intensity: $1.0\text{ W}/\text{cm}^2$) was fixed at the bottom of thermostatic water bath. The cell culture plate was suspended 3 cm above the ultrasound transducer. Four groups were involved in this study. They are respectively the control group (HT(-)SDT(-)), the HT group (HT(+SDT(-)), the SDT group (HT (-)SDT(+)), and the HT plus SDT group (HT(+SDT(+)). HT treatment and SDT treatment were imposed simultaneously. The temperature of the water bath was 42°C with HT treatment lasting for 15 min and 37°C without HT treatment. The whole experiment was conducted in the dark to avoid PDT effect.

Animal tumor model and treatments *in vivo*

Five-week-old female BALB/c nude mice (Cavens Laboratory Animal Company, Changzhou, China) were fed in a specific pathogen-free device. U251 cell suspension (5×10^6 cells) was subcutaneously injected near the hip of the mice to induce solid tumors. When the tumor reached a volume of 100 mm^3 (about 12–14 days later), the mice were randomly divided into four groups ($n=5$ per group): the control group, the HT group, the SDT group, and the HT plus SDT group. The device of SDT plus HT used *in vivo* is the same as *in vitro* experiment (Fig. 1). The control group received no treatment, and the HT group received hyperthermotherapy through bathing at 42°C for 15 min. The mice of SDT group were treated intraperitoneally with 250 mg/kg 5-ALA and ultrasound of $2.0\text{ W}/\text{cm}^2$ for 10 min while the mice of SDT plus HT group were treated with SDT and HT. The treatments were performed every 3 days consecutively for 21 days, and the mice were kept away from light

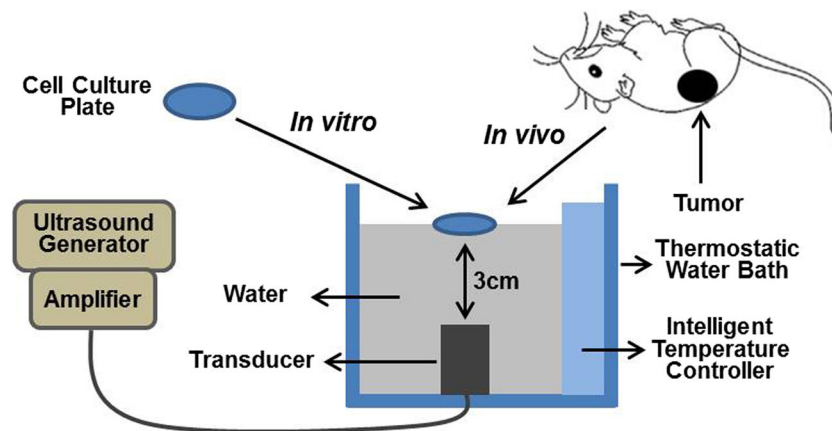


Fig. 1 Schematic diagram of the device of SDT plus HT

until the end of in vivo experiment. The tumor volumes were measured and calculated according to the formula: volume = length \times width \times width/2. All animal experimental protocols were approved of by Medical Ethics Committee of the Harbin Medical University.

Gaging of accumulation of protoporphyrin IX in glioma

5×10^5 cells were seeded in six-well plate and incubated for 24 h. 5-ALA was added at a final concentration of 0.5 mM after the medium was replaced with serum-free DMEM. Then, the cells were incubated and collected separately at 0, 2, 4, 6, 8, and 10 h after adding 5-ALA. Having been washed with PBS for twice, the collected cells were then centrifuged into pellets. Then, the fluorescence spectral of PpIX was immediately detected using the spectrometer which works with 405 nm excitation and 390–800 nm emission. A sharp peak representing the strength of fluorescence was detected at 636 nm emission (VLD-EX, SBI Pharmaceuticals Co., Ltd., Tokyo, Japan). And its intensity data were analyzed with Spectrometer Data Acquisition Software (BWSpec 3.26_14, Newark, DE, USA).

Preparation for characterization of the cell morphology

SNB19 and U87MG cells were under the same treatment respectively as what was described previously in the cell viability assay. After 24-h incubation in the dark, the morphology and adherent growth of cells were observed with an inverted microscope (Olympus IX71, Olympus, Tokyo, Japan).

Cell viability assay

In line with earlier description, Alamar blue assay was utilized to assess cell viability [25]. 5×10^5 cells seeded into six-well microplates were incubated for 12 h and then treated with DMEM containing 0.5 mM 5-ALA for 6 h in the dark. The medium was replaced with DMEM supplemented with 10 %

FBS. Afterwards, the cells were exposed to ultrasound at 1 MHz, 1.0 W/cm^2 for 2 min, and HT by bathing at 42°C for 15 min as described above. After incubation for 24 h at 37°C , 1000 cells of each population were seeded in 96-well microplates in 200 μl of culture medium containing 0.1 % FBS. The plates underwent incubation for 4 h at 37°C , and a 20 μl volume of alamar blue (which is 10 % of the total) was added to the cells and incubated. The plate was read using a microplate reader (double filters: 570 nm, 595 nm) at 24, 48, 72, and 96 h. Average absorbance values were calculated.

Cell apoptosis analysis in vitro

Annexin V-FITC apoptosis detection kit was used to analyze cell apoptosis in this study. Twelve hours after HT and SDT treatments, the glioma cells of various groups were separately harvested, washed, and pelleted by centrifugation. Then, the cells were suspended in 1 ml $1 \times$ Binding Buffer, which was removed from the cell pellet after $600 \times g$ centrifugation for 10 min. One hundred microliters of cells (about 1×10^5 cells per test) was added to each labeled tube. Five microliters of Annexin V-FITC and 5 μl of propidium iodide (PI) were added to appropriate tubes, which were rocked gently and incubated for 10 min at room temperature, protected from light. Four hundred microliters of PBS was added into the tube and rocked gently. At least 1×10^4 stained cells were analyzed by BD FACSVerse system (Becton Dickinson, Bedford, MA, USA) in 1 hour. The data were analyzed with BD CellQuest™ Pro Software.

TUNEL assay of apoptotic cells in vivo

The terminal deoxyribonucleotide transferase-mediated nick-end labeling (TUNEL) assay kit (Roche, Switzerland) was used to assess the cell apoptosis in the tumor tissues. The apoptotic index was calculated by dividing the number of TUNEL-positive cells (tan or brown stained) by the total

number of cells from 10 high-power fields (magnification $\times 400$) which were randomly selected.

Mitochondrial membrane potential detection

Cationic cyanine dyes have been shown to accumulate in cells in response to MMP, and their change has been studied in association with apoptosis. MitoProbe™ DiIC1(5) assay kit was used to analyze MMP. The glioma cells underwent the same treatment as performed previously in the cell apoptosis assay. After incubation with DMEM supplemented with 10 % FBS for 6 h at 37 °C, all the cells were collected, pelleted by centrifugation, and suspended in 1 ml warm (37 °C) DMEM at approximately 1×10^6 cells/ml. Five microliters of DiIC1(5) was added to the cells, which was incubated at 37 °C, 5 % CO₂ for 20 min in the dark. The cells were washed once with warm PBS, pelleted, and resuspended in 500 μ l PBS. The stained cells were visualized on BD FACSVerser system with red excitation and far red emission.

Intracellular ROS detection

Intracellular ROS was assessed using CellROX® Green Flow Cytometry Assay Kit. Though essentially non-fluorescent in a reduced state, the cell-permeable CellROX® reagent exhibits a strong fluorogenic signal upon oxidation, providing a reliable measure of ROS in live cells. Two hours after 5-ALA-SDT and HT treatment, the glioma cells were labeled with CellROX® Green Flow Cytometry Assay Kit according to the manufacturer's instructions. And then ROS was analyzed on BD FACSVerser flow cytometer in 1 hour. The data were analyzed with Cell Quest software.

Immunoblot analysis

To characterize the apoptotic signals and potential mechanism much further, expressions of apoptosis-related proteins, including cleaved caspase-3, cleaved caspase-8, cleaved caspase-9, Bax, and Bcl-2, were detected with Western blot. Twenty hours after HT and SDT treatments, SNB19 and U87MG cells of various groups were separately washed, collected, and lysed with lysis buffer according to the manufacturer's procedures. The target proteins were analyzed by SDS-PAGE followed by Western blotting utilizing specific primary antibody (Wanleibio, Shenyang, China) and secondary antibodies, respectively. In order to warrant equal loading, mouse antibody specific to human β -actin was used. Finally, chemiluminescence yielded from substrates of photographs was captured, and images were quantified using Image J software (NIH, Maryland, USA).

Immunohistochemistry

The tumor tissues fixed in 4 % paraformaldehyde were dehydrated with graded ethanol and paraffin embedded. After being deparaffined, rehydrated, the tumor tissue sections (4 μ m) were heated in citrate buffer for 15 min for antigen retrieval. Endogenous peroxidase of the tumor tissue was blocked with 3 % H₂O₂ at room temperature. The sections were blocked and stained with rabbit polyclonal anti-Bax (1:200), anti-Bcl-2 (1:400), anti-cleaved caspase-3, 8, and 9 (1:400) (ProteinTech Group, Chicago, IL, USA) at 4 °C overnight. The primary antibodies were identified with goat anti-rabbit secondary antibodies and washed with PBS, followed by visualizing with DAB. Afterwards, the sections were counterstained with hematoxylin. Finally, the sections were scanned under a light microscopy at high-power fields (magnification $\times 400$). Image Pro Plus software 6.0 (Media Cybernetics, Bethesda, MD, USA) was utilized to quantify the extent of immunopositive expression of tumor cells with integrated optical density (IOD) values.

Statistical analysis

All data were expressed as mean \pm standard deviation (SD). One-way ANOVA, Dunnett *t* and LSD tests were used to determine statistical significance in the case of multiple comparisons. *P* value < 0.05 was considered significant.

Results

Intracellular accumulation of 5-ALA-PpIX

We confirmed intracellular accumulation of 5-ALA-PpIX in glioma cell lines with a spectrometer. The fluorescence spectrum data showed that there was a time-dependent intracellular accumulation of PpIX in glioma cell lines which were exposed to exogenous 5-ALA. A sharp peak at 636 nm, indicating the PpIX characteristic fluorescence spectra, was detected in SNB19 and U87MG cells in the study (Fig. 2a). The fluorescence intensity of PpIX increased in a time-dependent manner in both cell lines after being incubated with a final concentration of 0.5 mM 5-ALA, peaked at 8 h, and then weakened with the passage of time (Fig. 2b). The accumulation of PpIX in U87MG cells was much higher than that in SNB19 cells under the same conditions, implying that U87MG cells are more sensitive to exogenous 5-ALA than SNB19 cells.

Effect of SDT and HT on the morphology in glioma cells

The morphology and adherent growth of SNB19 (Fig. 3a) and U87MG (Fig. 3b) cells were observed 24 h after the four

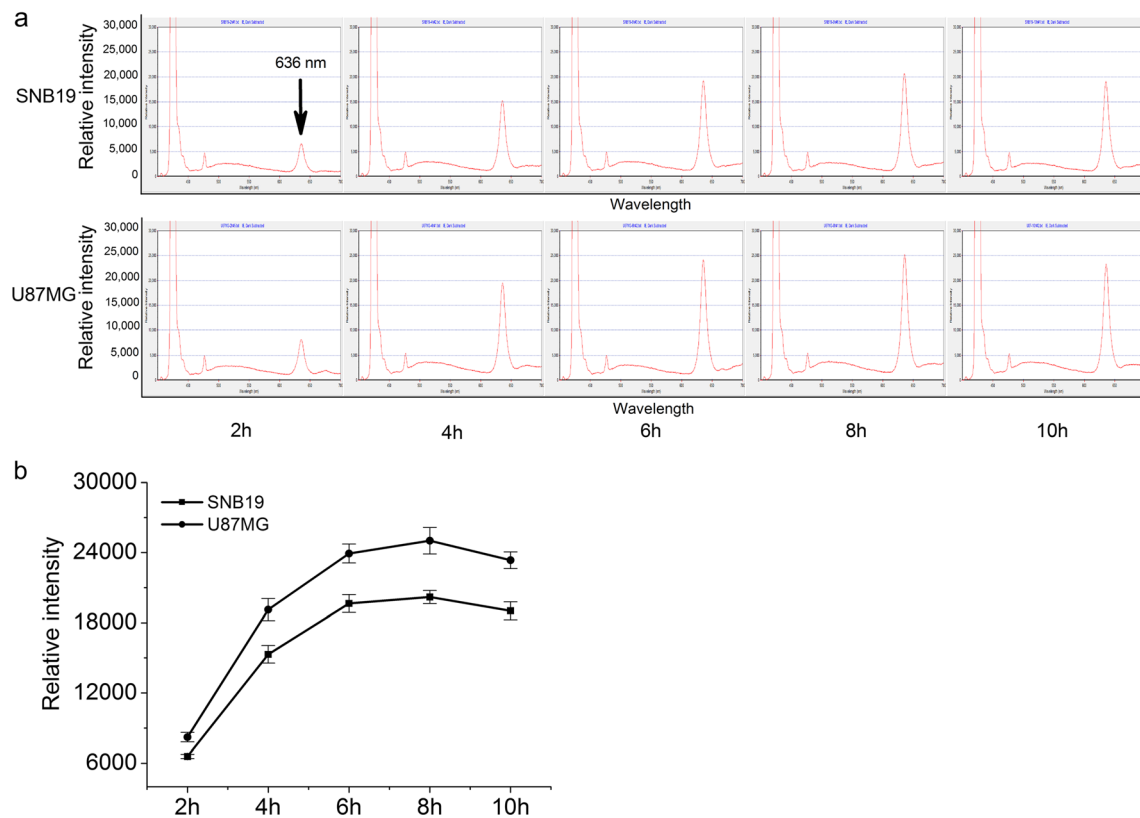


Fig. 2 Accumulation of PpIX in glioma cells after 5-ALA exposure. **a** PpIX fluorescence spectra tracing at various time points. The peak at 636 nm (arrow) indicates the PpIX characteristic fluorescence spectra. x axis: wavelength, y axis: relative intensity. **b** The time-dependent PpIX

accumulation curve was drawn according to the results of (a). PpIX fluorescence spectral intensity peaked at 8 h in both SNB19 and U87MG. Data represent the means \pm SD of individual groups ($n = 6$ per group)

different treatments using an inverted optical microscope. As shown in Fig. 3, control and HT groups showed adherently grown cells, which had good vitality and clear contour of fusiform and triquetrous shapes, while SDT and SDT plus HT groups showed poorly grown cells, which were not firmly attached or even suspended. And also, the part cells became circular.

Effect of SDT and HT on cell viability in glioma cells

To confirm the effect of combination of SDT and HT, we performed Alamar blue assay. According to the cell viability curve diagram, the cells treated with SDT and SDT plus HT both showed an obvious inhibitory action on cell viability in both SNB19 and U87MG cells. Moreover, cell viability was much more suppressed with SDT plus HT than with SDT in both cell lines (Fig. 4a, b). Alamar blue assay also showed that cell viability was affected by temperature, 5-ALA concentration, and ultrasound exposure time. As shown in Fig. 4c, d, e, U87MG cell viability decreased significantly with the increase of 5-ALA concentration (0.1–1.0 mM) in cells treated with SDT plus HT, by ultrasonic irradiation for 2 min and 42 °C lasting for 15 min; with the increase of ultrasound exposure

time (1–4 min) in cells treated with SDT plus HT, by 0.5 mM of 5-ALA concentration and 42 °C lasting for 15 min; with the increase of temperature (37–45 °C) in cells treated with SDT plus HT, by ultrasonic irradiation for 2 min and 0.5 mM of 5-ALA concentration. Similar results were also obtained in the case of SNB19.

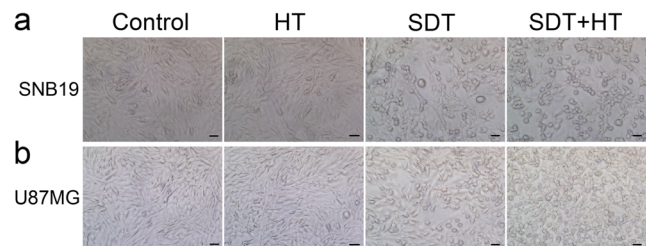


Fig. 3 Effect of SDT and HT on the morphology of glioma cells. The morphology and adherent growth of SNB19 (a) and U87MG (b) cells were observed 24 h after the four different treatments by an inverted optical microscope (Olympus IX71). Control and HT groups showed adherently grown cells, which had good vitality and clear contour of fusiform and triquetrous shapes, while SDT and SDT plus HT groups showed poorly grown cells, which were not firmly attached or even suspended. Also, the part cells became circular. Scale bars = 50 μ m ($\times 200$)

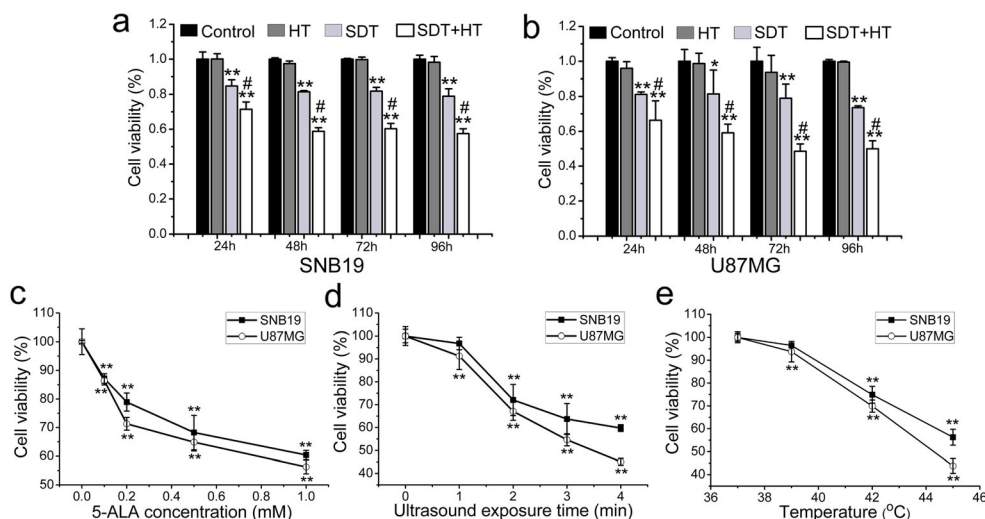


Fig. 4 Effect of SDT and HT on the cell viability in glioma cells. **a** SNB19 and **b** U87MG cells were exposed to ultrasound for 2 min at 5-ALA concentrations of 0.5 mmol/L and HT by bathing at 42 °C for 15 min. **c** Glioma cells were exposed to ultrasound for 2 min at 5-ALA concentrations of 0, 0.1, 0.2, 0.5, and 1.0 mmol/L and HT by bathing at 42 °C for 15 min. **d** Glioma cells were exposed to ultrasound for 0, 1, 2, 3,

and 4 min at 5-ALA concentrations of 0.5 mmol/L and HT by bathing at 42 °C for 15 min. **e** Glioma cells were exposed to ultrasound for 2 min at 5-ALA concentrations of 0.5 mmol/L and HT by bathing at 37, 39, 42, and 45 °C for 15 min. Data represent the means \pm SD of individual groups (* P < 0.05, ** P < 0.01 vs. the control group or the HT group. # P < 0.05 vs. the SDT group)

Antitumor effect of SDT and HT in vivo

To explore whether HT affects the antitumor efficacy of SDT against human glioma cells in vivo, we observed the effect of SDT in combination with HT on the growth of human glioma transplanted subcutaneously in nude mice. Figure 5a shows the difference of tumor volumes at 21 days after each treatment. As shown in Fig. 5b, the growth curve of xenografts showed that the HT groups experienced no significant difference in tumor growth compared with the control group, while the SDT group and the SDT plus HT group exhibited significantly lower tumor growth compared with the other groups (P < 0.01). Furthermore, the tumor volume in HT plus SDT group is much smaller compared with SDT group (P < 0.05). The increase in tumor volume was greater than 15-fold in the control group and the HT group, greater than fivefold in the SDT groups, but less than threefold in the SDT group. These data indicate that HT enhances SDT-modulated tumor growth delay in glioma in vivo.

Cell apoptosis after SDT + HT in glioma

We then investigated whether hyperthermotherapy influences cell apoptosis induced by SDT. For in vitro case, cell apoptosis was quantified by flow cytometry using double staining of Annexin V and PI. The results showed that apoptotic rate in control group and HT group (42 °C lasting for 15 min) was almost parallel (SNB19 P = 0.924, U87MG P = 0.475), while more apoptotic cells were observed in both SDT group and HT plus SDT group in both U87MG and SNB19 cells. Furthermore, apoptotic rate of both early and late apoptotic

cell in HT plus SDT group was much higher than in SDT group, since cells that are in late apoptosis are both Annexin V- and PI-positive, while cells that are in early apoptosis are Annexin V-positive and PI-negative (Fig. 6). Additionally, the rate of U87MG (42.8 \pm 12.6 %) was higher than SNB19 (21.0 \pm 1.6 %) in HT plus SDT group under the same conditions, reflecting that U87MG cells are more sensitive to combination of 5-ALA-SDT and HT than SNB19 cells. For in vivo case, cell apoptosis was detected by TUNEL assay. As shown in Fig. 5c, a few of stained cells were observed in control group and HT group, whereas more apoptotic cells unevenly distributed in the transplant tumor were observed perceptibly in SDT group and SDT plus HT group. More importantly, the score of TUNEL in SDT plus HT group was much higher than that in SDT group (Fig. 5d, P < 0.05). Taken together, these data indicate that HT enhances SDT-modulated cell apoptosis in glioma both in vitro and in vivo.

Loss of MMP after SDT + HT in glioma cells

In order to test cell apoptosis, loss of mitochondrial membrane potential was assessed using MitoProbe™ DiIC1(5) assay. As illustrated in Fig. 7, the level of MMP of HT group was not different from that of the control group in both U87MG and SNB19 cells (SNB19 P = 0.547, U87MG P = 0.220). However, the level of MMP of SDT group and HT plus SDT group was decreased remarkably (SNB19 P = 0.000, U87MG P = 0.000; Fig. 7). The results also showed that there was a distinct loss of MMP in HT plus SDT group in both glioma cell lines, compared with SDT group.

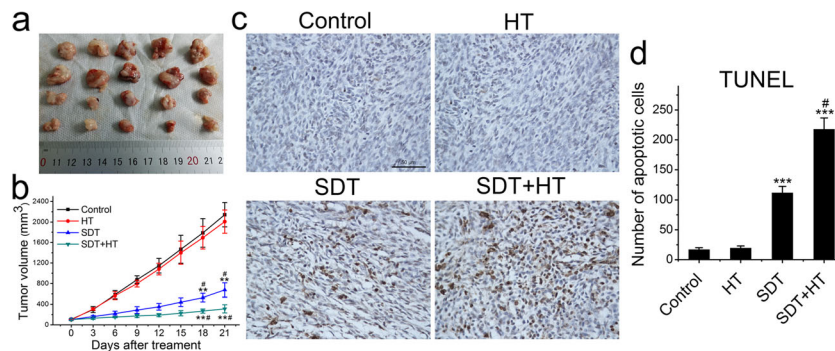


Fig. 5 Inhibitory effect of SDT and HT on tumor growth and TUNEL assay in U251 xenograft tumors. **a** Photograph showing excised tumors in representative nude mice in each group implanted with U251 cells ($n = 5$ mice per treatment group) on day 21 after treatment. **b** Growth curve of the xenograft tumors. **c** The TUNEL analysis of apoptotic cells in the

tumors. **d** The Quantitative analysis of apoptotic tumor cells. Data represent the means \pm SD of individual groups (** $P < 0.01$, *** $P < 0.005$ vs. the Control group or the HT group. # $P < 0.05$ vs. the SDT group). Scale bars = 50 μ m ($\times 400$)

Production of ROS after SDT + HT in glioma cells

In subsequent experiments, production of ROS induced by SDT was measured by flow cytometric analysis using CellROX[®] Green Flow Cytometry Assay Kit. The cells in the lower-right quadrant represent the cells which generated ROS. The results showed that percentage of the cells which had generated ROS in control group and HT group (42 °C lasting for 15 min) was

almost identical (SNB19 $P = 0.988$, U87MG $P = 0.995$), while much more ROS production was detected in both SDT group and HT plus SDT group in both U87MG and SNB19 cells (Fig. 8). Furthermore, compared with SDT group, there were more cells which had generated ROS in HT plus SDT group in both cell lines (SNB19 $P = 0.005$, U87MG $P = 0.007$; Fig. 8). These data suggest that HT promoted the generation of ROS induced by 5-ALA-SDT in both cell lines.

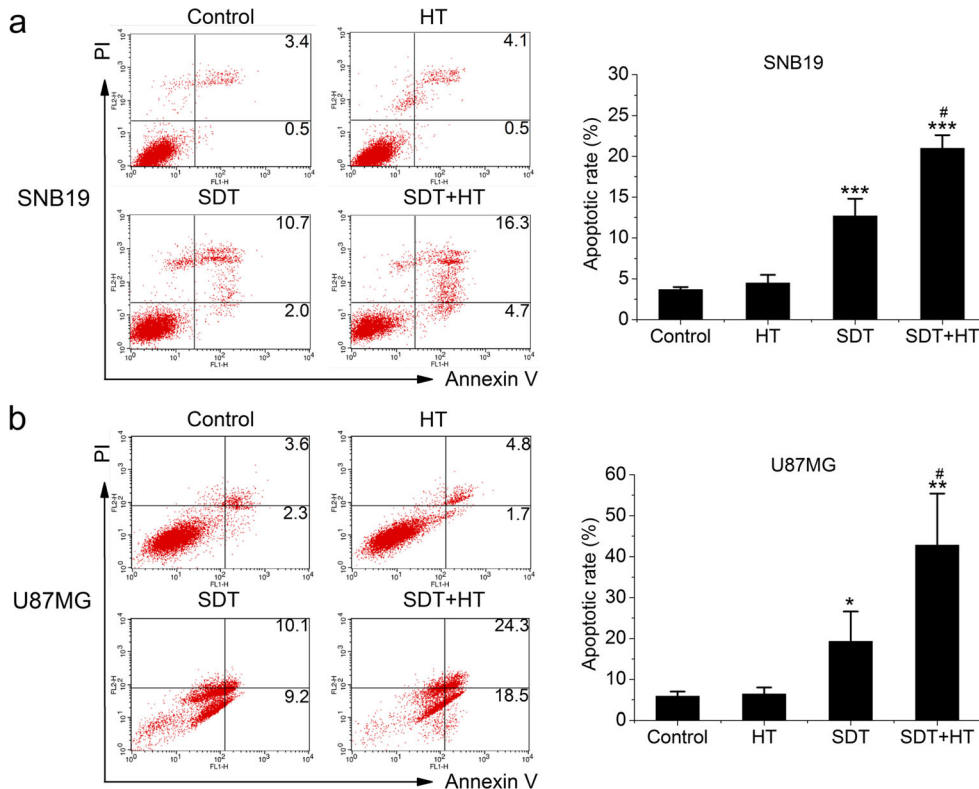


Fig. 6 Effect of SDT plus HT on the cell apoptosis in glioma cells. Apoptotic rate of both early and late apoptotic cell in HT plus SDT group at 12 h after 5-ALA-SDT plus HT was much higher than in SDT only group in SNB19 (a) and U87MG (b) cells. Data represent the means

\pm SD ($n = 4$ per group, * $P < 0.05$, ** $P < 0.01$, *** $P < 0.005$ vs. the control group or the HT group. # $P < 0.05$ vs. the SDT group). Note: Cells that are in early apoptosis are Annexin V-positive and PI-negative, and cells that are in late apoptosis are both Annexin V- and PI-positive

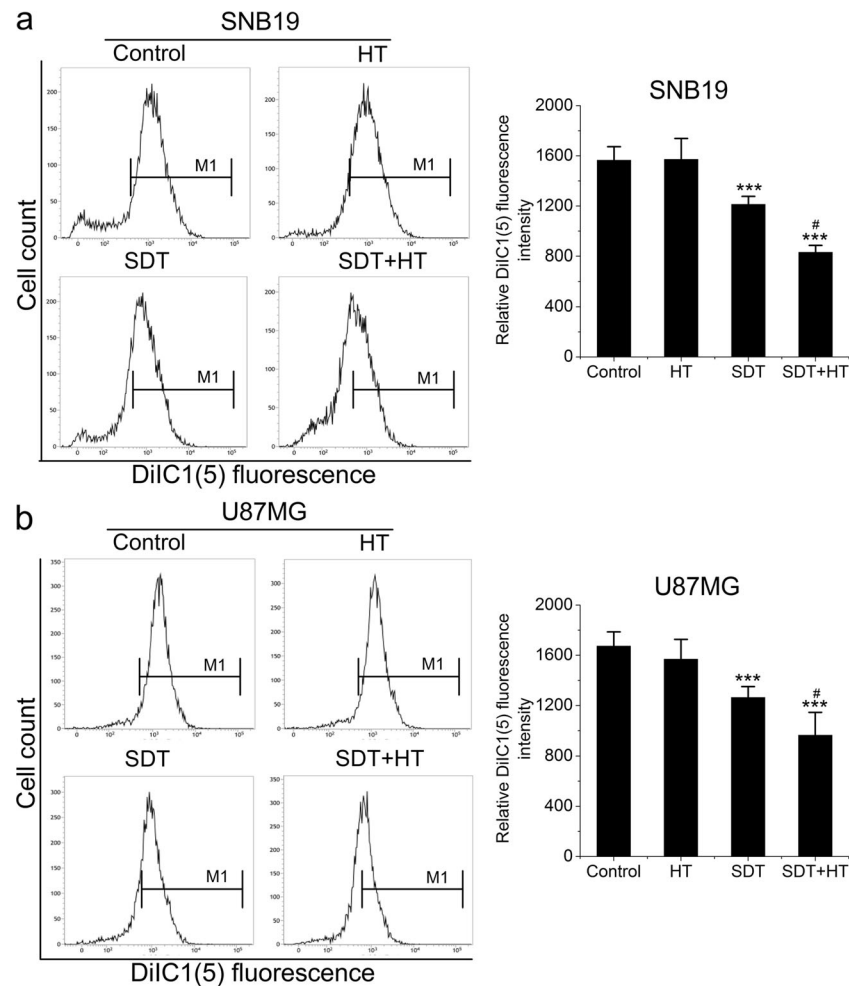


Fig. 7 Effect of SDT plus HT on the MMP loss in glioma cells. The level of MMP of SDT group and HT plus SDT group was decreased remarkably. And there was a distinct loss of MMP in HT plus SDT group in both SNB19 (a) and U87MG (b) cell lines, compared with

SDT group. Data represent the means \pm SD individual groups ($n=6$ per group, *** $P < 0.005$ vs. the control group or the HT group. # $P < 0.05$ vs. the SDT group)

Modulation of the expression of apoptosis-related proteins by SDT and HT in glioma

At the same time, we performed Western blot and immunohistochemistry to examine apoptosis-related proteins in order to explore the contribution of HT to 5-ALA-SDT. For in vitro case, Western blot analysis revealed that the expressions of cleaved caspase-3, 8, 9, and Bax were upregulated but Bcl-2 was downregulated in SNB19 and U87MG cells treated with SDT and SDT plus HT, as compared with those in non-treated cells (Fig. 9). Moreover, HT upregulated the expression of cleaved caspase-3, 8, 9, and Bax and downregulated the expression of Bcl-2 in SDT plus HT group in both cell lines, as compared with those in SDT group (Fig. 9). For in vivo case, similar results were also obtained in the case of immunohistochemistry (Fig. 10). Taken together, these data suggest that HT enhanced the expression of pro-apoptotic proteins and inhibits anti-apoptotic proteins, thus promoting apoptosis induced by SDT of glioma both in vitro and in vivo.

Discussion

In our study we proposed to use SDT in combination with HT for human malignant glioma treatment, and found that HT improved antitumor effects induced by 5-ALA-SDT in glioma both in vitro and in vivo. However, this degree of heat stress did not affect the tumor growth of human glioma. We found that SDT in combination with HT significantly decreased the cell viability, compared with SDT, and the viability was decreased depending on the raise of 5-ALA concentration, ultrasound exposure time, and temperature. Meanwhile, the results indicate that HT increased a conspicuous apoptosis, ROS production, and a remarkable loss in MMP induced by 5-ALA-SDT. Furthermore, the mechanism involved partly the apoptosis induced by SDT in combination with HT through upregulation of the expression of Bax, downregulation of Bcl-2, and activation of caspase-3, 8, and 9.

Here, we confirmed that intracellular PpIX preferentially accumulated with a time-dependent in glioma cell lines

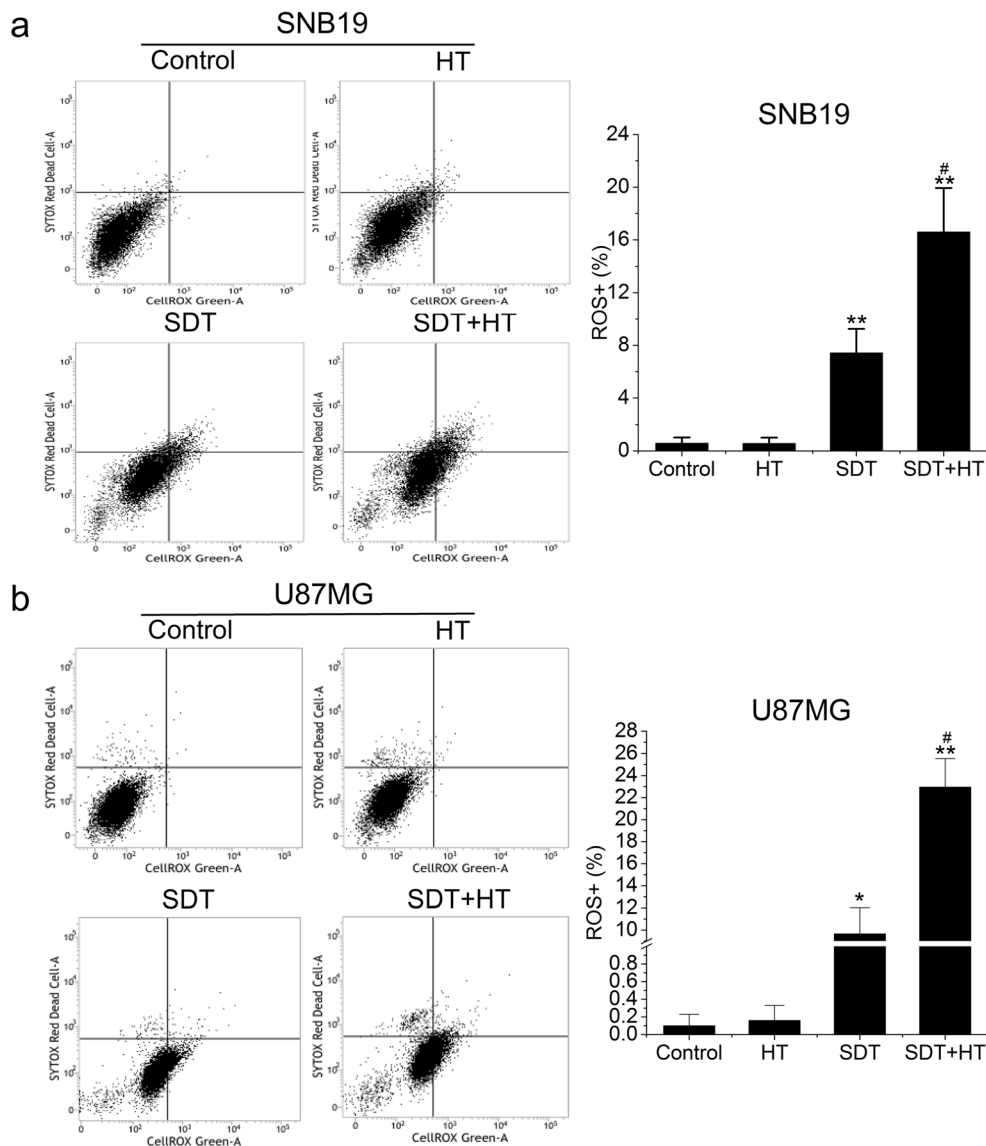


Fig. 8 Effect of SDT plus HT on the ROS generation in glioma cells. The percentage of ROS-producing cells in SDT group and HT plus SDT group increased remarkably. And there was an obvious rise of ROS generation in HT plus SDT group in both SNB19 (a) and U87MG (b) cell

lines, compared with SDT group. Data represent the means \pm SD individual groups ($n = 6$ per group, * $P < 0.05$, ** $P < 0.01$ vs. the control group or the HT group. # $P < 0.05$ vs. the SDT group)

through the administration of 5-ALA. The accumulation of PpIX in U87MG cells was much higher than that in SNB19 cells under the same conditions, implying that U87MG cells are more sensitive to exogenous 5-ALA than SNB19 cells. The results are consistent with the previous report [25]. Furthermore, cell viability was measured by Alamar blue assay after 5-ALA-SDT. We found that HT significantly decreased viability of cells treated with 5-ALA-SDT, and the effect increased with 5-ALA concentration, ultrasound exposure time, and temperature. Meanwhile, our data also indicate that HT enhances SDT-modulated tumor growth delay in glioma in vivo. The difference of the accumulation amount of PpIX between SNB19 and U87MG may result in the response of cell viability, tumor growth, apoptosis, and pro-apoptotic

protein since PpIX level influences cell toxicity by the SDT in a dose-dependent manner [26].

In order to gain an insight into the mechanism of synergism, the mode of cell death was determined as a function of treatment modality. Since SDT came into existence, a plethora of research has proved its antitumor function for a variety of cancer cells. As is shown in recent studies, the ways SDT works include inducing necrosis, apoptosis, autophagy, and so forth, and apoptosis is the salient form of cell death resulting from SDT for many cancer cells [21, 27, 28]. Compared with necrosis, apoptosis is clinically preferred as it will cause less inflammation reactions [29]. In this study, we further performed flow cytometry analysis and TUNEL assay to quantify cell apoptosis in glioma. As illustrated in Figs. 5

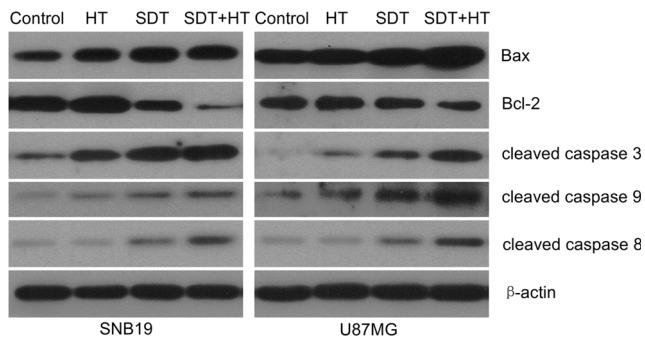


Fig. 9 SDT and HT modulates the expression of apoptosis-related proteins in glioma in vitro. Apoptosis-related proteins were detected with Western blotting utilizing specific antibodies, respectively. β -actin was used as loading control. Hyperthermotherapy upregulated the expression of cleaved caspase-3, 8, 9, and Bax and downregulated the expression of Bcl-2 in SDT plus HT group in SNB19 and U87MG cell lines

and 6, the cell apoptosis was obviously observed in SDT-treated cells, which was in accordance with previous studies on the SDT treatment of other cancer cells [17, 21–23]. Specifically, we clearly observed the cell apoptosis rate of the SDT plus HT group was much higher than that of the SDT group, while HT is a feeble inducer of apoptosis in glioma both in vitro and in vivo. Furthermore, late apoptosis was dominant over early apoptosis in SDT group and SDT plus HT group in vitro. As a consequence, these results indicated that the apoptosis induced by 5-ALA-SDT was obviously promoted by HT in glioma. To our

knowledge, although the results are in good agreement with the other findings that concurrent hyperthermia could enhance efficiency of PDT for the treatment of cancer [30, 31], the combined effects of SDT and HT have not been investigated.

Research in recent decades has revealed that the formation of normal MMP is requisite for maintaining the function of mitochondria [31, 32]. The loss in MMP could inhibit the function of mitochondrial adenosine triphosphate synthesis [33]. In the process of cell apoptosis induced by loss in MMP, which occurs earlier than DNA fragmentation and cell membrane phosphatidylserine extroversion, is a symbolic and early signal on mitochondrial pathway [22, 34]. Similar to cell apoptosis, with flow cytometric analysis, loss in MMP was obviously observed in the experiment. We found that the cells treated by ALA-SDT displayed a decrease in MMP, and this decrease was remarkably enhanced in the presence of HT, which had little effect working alone. As such, these results suggested that HT played a role in accelerating mitochondrial dysfunction induced by SDT in the apoptotic pathway.

ROS refers to the oxygen-containing atom or atomic group that has active chemical property. It is well known that encompassing multiple types such as oxygen-free radical, hydroxyl radical, hydrogen peroxide, and H_2O_2 , ROS participate in various physiological and pathologic processes including cell proliferation, differentiation, senility, and apoptosis [35, 36]. When cells undergo various exogenous stimulants such as ionizing radiation, heat stress, and chemotherapy drugs, excessive

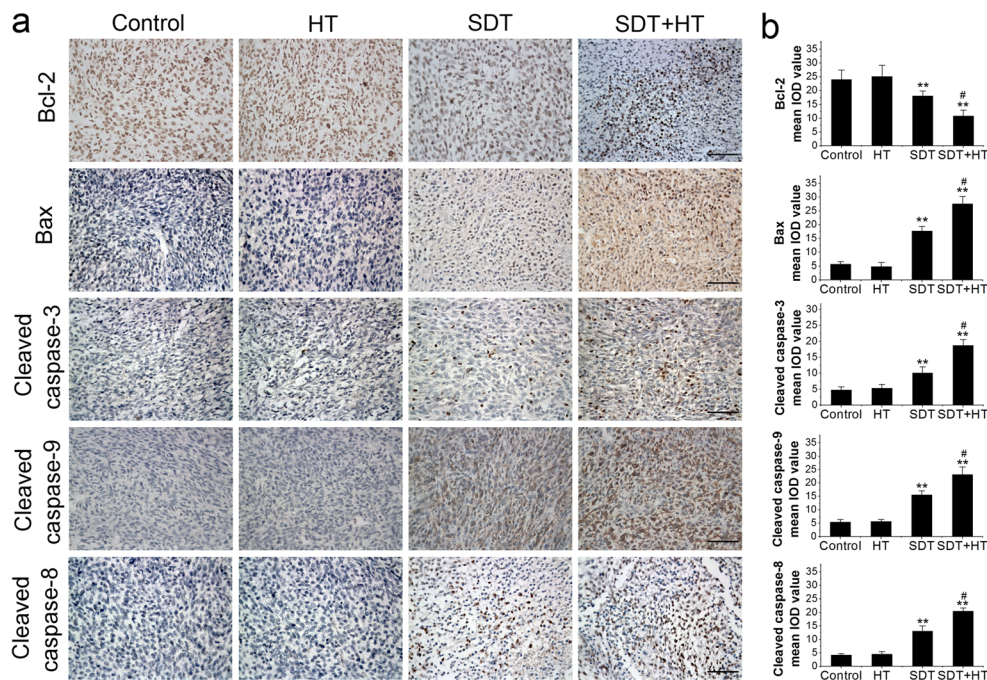


Fig. 10 SDT and HT modulates the expression of apoptosis-related proteins in glioma in vivo. Apoptosis-related proteins were detected with immunohistochemistry using specific antibodies, respectively. Hyperthermotherapy upregulated the expression of cleaved caspase-3, 8, 9, and Bax and downregulated the expression of Bcl-2 in the SDT plus HT group in vivo. **a**

Immunohistochemistry analysis. **b** Quantitative analysis of the IOD values. Data represent the means \pm SD individual groups ($n = 5$ per group, $**P < 0.01$ vs. the control group or the HT group, $\#P < 0.05$ vs. the SDT group). Scale bars = 50 μ m ($\times 400$)

amount of ROS will be produced to cause oxidative stress inside the cells, which consequently will lead to cell trauma or death [36, 37]. A growing body of evidence suggests that SDT can induce cancer cells to produce a surplus of ROS, which selectively kills cancer cells through inducing cell apoptosis, death, or autophagy [20, 22, 37]. A group of researches in recent years have proved heat stress can cause an explosion of ROS inside the cells and can directly cause cell apoptosis [38–40]. We found an interesting phenomenon in the experiment: though 42 °C lasting for 15 min did not trigger ROS, it obviously promoted SDT to produce excessive amount of ROS. Combine this result with previous data, we propose that it is ROS induced by synergistic effect between 5-ALA-SDT and HT that has induced cell apoptosis and restrained cell proliferation.

Bcl-2 family is a group of key proteins that can control the mitochondria-mediated apoptosis [41]. They include Bax which promotes apoptosis and bcl-2 which restrains apoptosis. Located on the outer membrane of mitochondria, Bcl-2 can form Bax/Bcl-2 heterodimers with Bax, changing the permeability of the membrane of mitochondria [42]. Several studies have revealed that SDT modulates the expression of apoptosis-related proteins in tumor cells [22, 28]. In this study, we observed HT significantly increased the expression of cleaved caspase-3, 9, and Bax while decreased the expression of Bcl-2 in SDT plus HT group in glioma, as compared with those in SDT group. The data of in vitro and in vivo experiments suggest that the intrinsic apoptosis pathway might be an important mechanism responsible for apoptosis induced by SDT plus HT. Furthermore, we also found that cleaved caspase-8, which is closely related to extrinsic apoptosis pathway, was increased in SDT plus HT group. Although triggers of extrinsic apoptosis pathway, such as tumor necrosis factor (TNF), Fas ligand, TNF-related apoptosis-inducing ligand (TRAIL) were not investigated in this study, extrinsic apoptosis pathway may be accelerated by the combination of SDT and HT. Further experiments should be performed to clarify the involvement of extrinsic apoptosis pathway in SDT plus HT. As such, our study showed that HT may promote apoptosis induced by 5-ALA-SDT partly by activating caspases and modulating Bcl-2 family members.

Conclusion

In summary, we found that the enhancement of 5-ALA-SDT-induced cell apoptosis and tumor growth delay in human glioma both in vitro and in vivo experiments can be successfully achieved with HT, which does not influence the cell viability, apoptosis, and tumor growth of human glioma. Our data also indicate that HT increased conspicuous ROS production and a remarkable loss in MMP induced by 5-ALA-SDT in human glioma cell lines. In addition, this study also demonstrated that the mechanism involves, at least partially, modulating the

expression of apoptosis-related proteins and activating caspases may be closely related to the improved efficacy caused by SDT and HT in human glioma. The available findings may provide an important insight into SDT in combination with HT and further propose that SDT in combination with HT is a new potential application for the treatment of human glioma.

Acknowledgments We are grateful to Atsushi Chuma, Ito Co., LTD. for kindly providing ultrasonic apparatus. Miyuki Takatori and Kiyomi Kikukawa, Research Center for Life Science, Nippon Medical School, provided technical supports for the flow-cytometric analysis. We are also grateful to Ying Hu, School of Life Science and Technology, Harbin Institute of Technology, for providing technical assistance. This work was partly supported by Grant-in-Aid for challenging Exploratory Research from JSPS KAKENHI grant number 25670626 to FY. In addition, this work was also supported by grants from the Science and Technology Cooperation Project Foundation of Heilongjiang Medical Science Institute (ys14c11).

Compliance with ethical standards

Conflicts of interest None

References

1. Alifieris C, Trafalis DT. Glioblastoma multiforme: pathogenesis and treatment. *Pharmacol Ther.* 2015;152:63–82.
2. Wen PY, Kesari S. Malignant gliomas in adults. *N Engl J Med.* 2008;359(5):492–507.
3. Paw I, Carpenter RC, Watabe K, Debinski W, Lo HW. Mechanisms regulating glioma invasion. *Cancer Lett.* 2015;362(1):1–7.
4. Gállego Pérez-Larraya J, Delattre JY. Management of elderly patients with gliomas. *Oncologist.* 2014;19(12):1258–67.
5. Juratli TA, Schackert G, Krex D. Current status of local therapy in malignant gliomas—a clinical review of three selected approaches. *Pharmacol Ther.* 2013;139(3):341–58.
6. Arrillaga-Romany I, Reardon DA, Wen PY. Current status of antiangiogenic therapies for glioblastomas. *Expert Opin Investig Drugs.* 2014;23(2):199–210.
7. Stupp R, Hegi ME, Mason WP, van den Bent MJ, Taphoorn MJ, Janzer RC, et al. Effects of radiotherapy with concomitant and adjuvant temozolomide versus radiotherapy alone on survival in glioblastoma in a randomised phase III study: 5-year analysis of the EORTC-NCIC trial. *Lancet Oncol.* 2009;10(5):459–66.
8. Falk MH, Issels RD. Hyperthermia in oncology. *Int J Hypertherm.* 2001;17(1):1–18.
9. Yi GQ, Gu B, Chen LK. The safety and efficacy of magnetic nano-iron hyperthermia therapy on rat brain glioma. *Tumor Biol.* 2014;35(3):2445–9.
10. Otte J. Hyperthermia in cancer therapy. *Eur J Pediatr.* 1988;147(6):560–9.
11. Toraya-Brown S, Fiering S. Local tumor hyperthermia as immunotherapy for metastatic cancer. *Int J Hypertherm.* 2014;30(8):531–9.
12. Müller S. Magnetic fluid hyperthermia therapy for malignant brain tumors—an ethical discussion. *Nanomedicine.* 2009;5(4):387–93.
13. Mallory M, Gogineni E, Jones GC, Greer L, Simone CB 2nd. Therapeutic hyperthermia: The old, the new, and the upcoming.

- Crit Rev Oncol Hematol. 2015. doi:10.1016/j.critrevonc.2015.08.003.
14. Rao W, Deng ZS, Liu J. A review of hyperthermia combined with radiotherapy/chemotherapy on malignant tumors. *Crit Rev Biomed Eng.* 2010;38(1):101–16.
 15. Inoue H, Kajimoto Y, Shibata MA, Miyoshi N, Ogawa N, Miyatake S, et al. Massive apoptotic cell death of human glioma cells via a mitochondrial pathway following 5-aminolevulinic acid-mediated photodynamic therapy. *J Neurooncol.* 2007;83(3):223–31.
 16. Krammer B, Plaetzer K. ALA and its clinical impact, from bench to bedside. *Photochem Photobiol Sci.* 2008;7(3):283–9.
 17. Gao Z, Zheng J, Yang B, Wang Z, Fan H, Lv Y, et al. Sonodynamic therapy inhibits angiogenesis and tumor growth in a xenograft mouse model. *Cancer Lett.* 2013;335(1):93–9.
 18. Yamaguchi F, Asakura T, Takahashi H, Kitamura T, Teramoto A. Low frequency ultrasonication induced antitumor effect in 5-Aminolevulinic acid treated malignant glioma. *J Cancer Ther.* 2013;4(1):170–5.
 19. Umemura S, Yumita N, Nishigaki R, Umemura K. Mechanism of cell damage by ultrasound in combination with hematoporphyrin. *Jpn J Cancer Res.* 1990;81(9):962–6.
 20. Tsuru H, Shibaguchi H, Kuroki M, Yamashita Y, Kuroki M. Tumor growth inhibition by sonodynamic therapy using a novel sonosensitizer. *Free Radic Biol Med.* 2012;53(3):464–72.
 21. Song W, Cui H, Zhang R, Zheng J, Cao W. Apoptosis of SAS cells induced by sonodynamic therapy using 5-aminolevulinic acid sonosensitizer. *Anticancer Res.* 2011;31(1):39–45.
 22. Wang H, Wang X, Zhang S, Wang P, Zhang K, Liu Q. Sinoporphyrin sodium, a novel sensitizer, triggers mitochondrial-dependent apoptosis in ECA-109 cells via production of reactive oxygen species. *Int J Nanomedicine.* 2014;9:3077–90.
 23. McEwan C, Owen J, Stride E, Fowley C, Nesbitt H, Cochrane D, et al. Oxygen carrying microbubbles for enhanced sonodynamic therapy of hypoxic tumors. *J Control Release.* 2015;203:51–6.
 24. Gross JL, Behrens DL, Mullins DE, Kornblith PL, Dexter DL. Plasminogen activator and inhibitor activity in human glioma cells and modulation by sodium butyrate. *Cancer Res.* 1988;48(2):291–6.
 25. Teng L, Nakada M, Zhao SG, Endo Y, Furuyama N, Nambu E, et al. Silencing of ferrochelatase enhances 5-aminolevulinic acid-based fluorescence and photodynamic therapy efficacy. *Br J Cancer.* 2011;104(5):798–807.
 26. Wang X, Jia Y, Su X, Wang P, Zhang K, Feng X, et al. Combination of protoporphyrin IX-mediated sonodynamic treatment with doxorubicin synergistically induced apoptotic cell death of a multidrug-resistant Leukemia K562/DOX cell line. *Ultrasound Med Biol.* 2015;41(10):2731–9.
 27. Canaparo R, Varchi G, Ballestri M, Foglietta F, Sotgiu G, Guerrini A, et al. Polymeric nanoparticles enhance the sonodynamic activity of meso-tetrakis (4-sulfonatophenyl) porphyrin in an vitro neuroblastoma model. *Int J Nanomedicine.* 2013;8:4247–63.
 28. Xiang J, Xia X, Jiang Y, Leung AW, Wang X, Xu J, et al. Apoptosis of ovarian cancer cells induced by methylene blue-mediated sonodynamic action. *Ultrasonics.* 2011;51(3):390–5.
 29. Dereski MO, Madigan L, Chopp M. The effect of hypothermia and hyperthermia on photodynamic therapy of normal brain. *Neurosurgery.* 1995;36(1):141–5.
 30. Chen B, Roskams T, de Witte PA. Enhancing the antitumoral effect of hypericin-mediated photodynamic therapy by hyperthermia. *Lasers Surg Med.* 2002;31(3):158–63.
 31. Lopez J, Tait SW. Mitochondrial apoptosis: killing cancer using the enemy within. *Br J Cancer.* 2015;112(6):957–62.
 32. Ly JD, Grubb DR, Lawen A. The mitochondrial membrane potential (deltapsi(m)) in apoptosis; an update. *Apoptosis.* 2003;8(2):115–28.
 33. Suski JM, Lebiecinska M, Bonora M, Pinton P, Duszynski J, Wieckowski MR. Relation between mitochondrial membrane potential and ROS formation. *Methods Mol Biol.* 2012;810:183–205.
 34. Gomez-Cabrera MC, Sanchis-Gomar F, Garcia-Valles R, Pareja-Galeano H, Gambini J, Borrás C, et al. Mitochondria as sources and targets of damage in cellular aging. *Clin Chem Lab Med.* 2012;50(8):1287–95.
 35. Trachootham D, Zhou Y, Zhang H, Demizu Y, Chen Z, Pelicano H, et al. Selective killing of oncogenically transformed cells through a ROS-mediated mechanism by beta-phenylethyl isothiocyanate. *Cancer Cell.* 2006;10(3):241–52.
 36. Dröge W. Free radicals in the physiological control of cell function. *Physiol Rev.* 2002;82:47–95.
 37. Trendowski M. The inherent metastasis of leukaemia and its exploitation by sonodynamic therapy. *Crit Rev Oncol Hematol.* 2015;94(2):149–63.
 38. Banerjee Mustafi S, Chakraborty PK, Dey RS, Raha S. Heat stress upregulates chaperone heat shock protein 70 and antioxidant manganese superoxide dismutase through reactive oxygen species (ROS), p38MAPK, and Akt. *Cell Stress Chaperones.* 2009;14(6):579–89.
 39. Zhang HJ, Xu L, Drake VJ, Xie L, Oberley LW, Kregel KC. Heat-induced liver injury in old rats is associated with exaggerated oxidative stress and altered transcription factor activation. *FASEB J.* 2003;17(15):2293–5.
 40. Palapati P, Averill-Bates DA. Mild thermotolerance induced at 40°C protects HeLa cells against activation of death receptor-mediated apoptosis by hydrogen peroxide. *Free Radic Biol Med.* 2011;50(6):667–79.
 41. Breckenridge DG, Xue D. Regulation of mitochondrial membrane permeabilization by Bcl-2 family proteins and caspases. *Curr Opin Cell Biol.* 2004;16(6):647–52.
 42. Schwarz CS, Evert BO, Seyfried J, Schaupp M, Kunz WS, Vielhaber S, et al. Overexpression of bcl-2 results in reduction of cytochrome c content and inhibition of complex I activity. *Biochem Biophys Res Commun.* 2001;280(4):1021–7.